

supplementary material

Table S1 Lat-lon boundary for the geographic regions in Fig. 1

Table S2. Effective sample size (N_e) for the spatial pattern correlation of AR frequency for each ocean basin.

Fig. S1. Time slice of AR tags detected using TE algorithm on (a) ERA5 and (b) BCC-CSM2 data on 1979-01-01T00

Fig. S2. Same as Fig. S1b but for AR tags detected by (a) ARCONNECT, (b) TECA, (c) Mundhenk and (d) Lora detection method.

Fig. S3. Time slice of AR tags detected using TE algorithm on (a) E3SM-LR and (b) E3SM-HR data on 1984-01-01T0

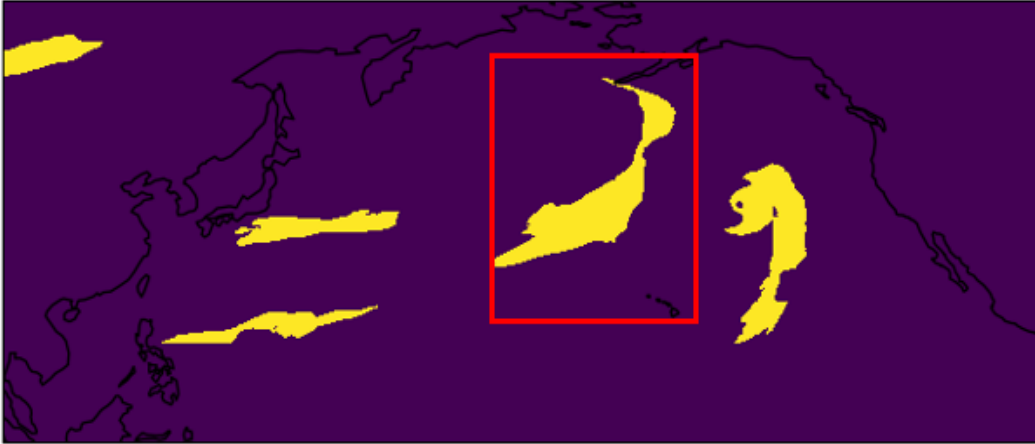
Table S1. Lat-Ion boundaries for geographic regions in Fig. 1

Region	S. Africa	Australia	New Zealand	S. America	Alaska	California	Baja	N. Europe	UK	Europe
Boundary	21-35.5°S 11-20°E	23-35.5°S 112.8-120°E	34-46.5°S 166-179°E	30-56°S 68-76°W	42-51°N 119-126°W	34-42°N 119-126°W	20-34°N 105-119°W	53-70°N 3.5-20°E	49.8-60°N 10°W - 2°E	35-49.8°N 10°W - 3.5°E
Region	W. Africa	Greenland	Antarctica	E. Asia	Pacific NW	N. Pacific	S. Pacific	N. Atlantic	S. Atlantic	Indian Ocean
Boundary	10-35°N 5-19°W	59.5- 67°N 40-52°W	60-76°S 57-95°W	31-43°N 125-142°E	42-51°N 119-126°W	0-67°N 99°E-98°W	0-70°S 142°E-70°W	0-75°N 80°W- 10°E	0-70°S 70°W-20°E	0-70°S 30-120°E

Table S2. Effective sample size (N_e) for the spatial pattern correlation of AR frequency for each ocean basin

	N. Pacific	S. Pacific	N. Atlantic	S. Atlantic	Indian Ocean
N_e	16	27	14	15	19

ERA5 1979-01-01T00



BCC 1979-01-01T00



Fig. S1. Time slice of AR tags detected using TE algorithm on (a) ERA5 and (b) BCC-CSM2 data on 1979-01-01T00

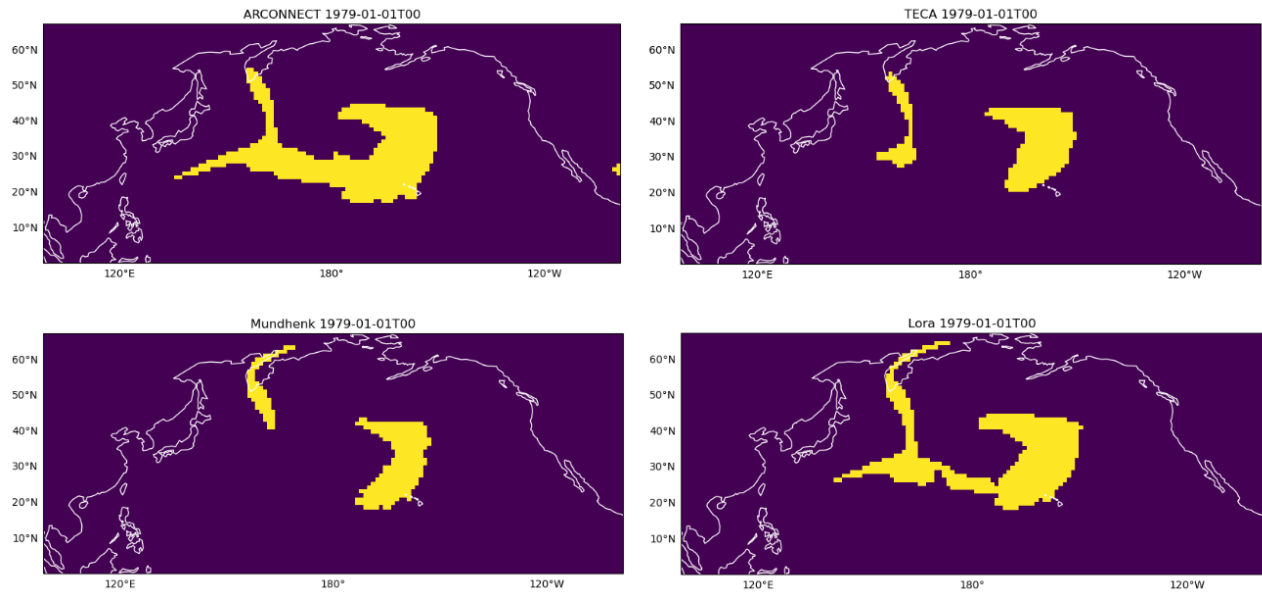


Fig. S2. Same as Fig. S1b but for AR tags detected by (a) ARCONNECT, (b) TECA, (c) Mundhenk and (d) Lora detection method.

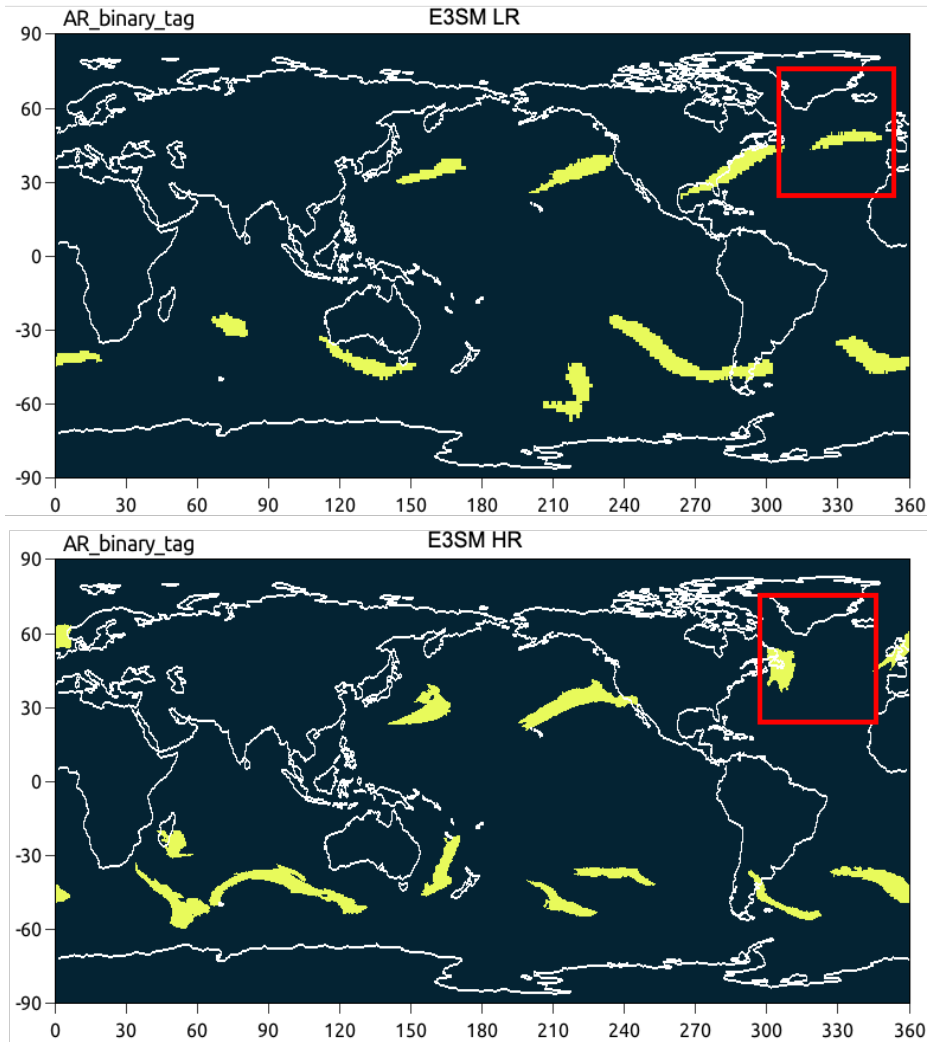


Fig. S3. Time slice of AR tags detected using TE algorithm on (a) E3SM-LR and (b) E3SM-HR data on 1984-01-01T00